URL: https://atvb-submit.aha-journals.org

Manuscript Number: ATVB/2017/309999D

Title: TGFβ blockade induces a human-like disease in a non-dissecting mouse model of abdominal aortic aneurysm

Authors: Fabien Lareyre (University of Cambridge), Marc Clément (University of Cambridge), Juliette Raffort (University of Cambridge), Stefanie Pohlod (Ecole Polytechnique Fédérale de Lausanne), Meghana Patel (University of Cambridge), Bruno Esposito (INSERM U970), Leanne Masters (University of Cambridge), Alison Finigan (University of Cambridge), Marie Vandestienne (INSERM U970), Nikolaos Stergiopulos (EPFL SV SSV-GE), Soraya Taleb (INSERM U970), Bram Trachet (Ecole Polytechnique Federale de Lausanne), and Ziad Mallat (University of Cambridge)

TGFβ blockade induces a human-like disease in a non-dissecting mouse model of abdominal aortic aneurysm

Lareyre, A human-like mouse model of AAA

Fabien Lareyre[1*], Marc Clément[1*], Juliette Raffort[1], Stefanie Pohlod[3], Meghana Patel[1], Bruno Esposito[2], Leanne Master[1], Alison Finigan[1], Marie Vandestienne[2], Nikolaos Stergiopulos[3,4], Soraya Taleb[2], Bram Trachet[3,4], Ziad Mallat[1,2]

[1]Division of Cardiovascular Medicine, University of Cambridge, Cambridge, UK.
[2]Institut National de la Santé et de la Recherche Médicale, Paris Cardiovascular Research Center, Paris, France
[3] Institute of Bioengineering, Ecole Polytechnique Fédérale de Lausanne, Lausanne, Switzerland
[4] IBiTech - bioMMeda, Ghent University, Ghent, Belgium

Correspondence to: Ziad Mallat, MD, PhD, at Division of Cardiovascular Medicine, University of Cambridge, Addenbrooke's Hospital, Cambridge, CB2 2QQ, UK. Tel: +44 1223 768678; E-Mail: zm255@medchl.cam.ac.uk.

*Equal contribution.
Total word count: 4866
Figures: 7
Subject codes: Pathophysiology; Aneurysm; Aortic Dissection.
OC category - Translational
TOC subcategory - Vascular Biology

Abstract

Objective — Current experimental models of abdominal aortic aneurysm (AAA) do not accurately reproduce the major features of human AAA. We hypothesized that blockade of TGFβ activity, a guardian of vascular integrity and immune homeostasis, would impair vascular healing in models of 'non-dissecting' AAA, and would lead to sustained aneurysmal growth until rupture.

Approach and Results — Here we test this hypothesis in the elastase-induced AAA model in mice. We analyze AAA development and progression using ultrasound in vivo, synchrotron-based ultrahigh resolution imaging ex-vivo, and a combination of biological, histological and flow cytometry-based cellular and molecular approaches in vitro. Systemic blockade of TGFβ using a monoclonal antibody induces a transition from a self-contained aortic dilatation to a model of sustained aneurysmal growth, associated with the formation of an intra-luminal thrombus (ILT). AAA growth is associated with wall disruption but no medial dissection, and culminates in fatal transmural aortic wall rupture. TGFβ blockade enhances leukocyte infiltration both in the aortic wall and the ILT, and aggravates extracellular matrix degradation. Early blockade of IL1β or monocyte-dependent responses substantially limits AAA severity. However, blockade of IL1β after disease initiation has no effect on AAA progression to rupture.

Conclusions — Endogenous TGFβ activity is required for the healing of AAA. TGFβ blockade may be harnessed to generate new models of AAA with better relevance to the human disease. We expect that the new models will improve our understanding of the pathophysiology of AAA, and will be useful in the identification of new therapeutic targets.

Abbreviations:

AAA: Abdominal aortic aneurysm
ILT: Intra-luminal thrombus
VSMC: vascular smooth muscle cell
ECM: Extracellular matrix
SatM: segregated-nucleus-containing atypical monocyte

Graphic Abstract

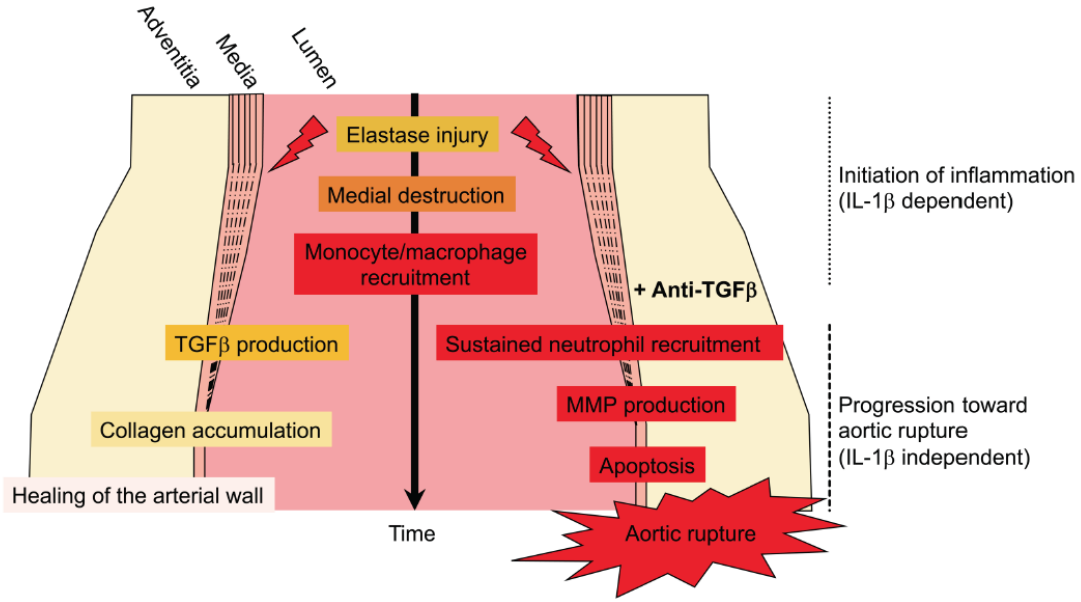

Introduction

The occurrence of abdominal aortic aneurysm (AAA) is a significant cause of morbidity and mortality in Western countries. According to the UK NHS AAA Screening Programme, the prevalence of AAA is 1.2% in all men at age 65 irrespective of any other risk factor [1]. AAA affects a much larger proportion of men over 65, particularly in the presence of a family history of AAA and a positive history of smoking [1,2]. In contrast, a history of diabetes is associated with a strong protection against the occurrence and progression of AAA [1-3]. AAA is responsible for more than 11,000 deaths/year in the USA and has been consistently found to resist medical treatment. Aortic wall repair through either endovascular or open surgical procedures is the only option available, with a relatively high risk of early or late morbidity and mortality [2,4].

The pathophysiology of AAA is complex and associates proteolysis of the extracellular matrix (ECM), degeneration and loss of vascular smooth muscle cells (VSMCs), alteration of endothelial cells and formation of intraluminal thrombus (ILT), along with an infiltration and activation of innate and adaptive immune cells [5]. The absence of resolution of those processes leads to progressive AAA growth, and culminates in AAA rupture when the aortic wall is unable to sustain the hemodynamic overload. Of note, in contrast to thoracic aortic aneurysms [6], medial dissection is a very rare event in AAA, which rather progress to a complete rupture of the thin aortic wall, usually at a stage of advanced aortic dilatation [7].

A variety of animal models have been developed to better understand the pathophysiology of AAA. Strikingly however, most models fail to reproduce or combine the major features of human AAA. Currently, most experimental models of AAA are performed in rodents, particularly mice, and can be divided in 2 main categories [8]. The first category includes models that induce medial aortic dissection rather than true aortic aneurysmal dilatation, and lead to hemorrhage into a false channel (intramural hemorrhage), which may ultimately rupture. This is the case of the angiotensin (Ang)II infusion model, initially described by the Daugherty and Cassis groups in mice with genetic susceptibility to hyperlipidemia and atherosclerosis [9,10], but also models of lysyl oxidase inhibition [11-13] and those combining mineralocorticoid receptor activation with high salt [14]. Despite the many advantages of those 'dissecting AAA' models, medial dissection is not a major feature of human AAA and is rarely an initiating event in the disease process [8]. Rather, most human AAAs are characterized by aneurysmal dilatation of the aorta without false channel formation, and culminate in a rupture of the thin aortic wall [7]. The second category of experimental AAAs includes models that induce abdominal aortic dilatation without medial dissection, as is the case for the widely used elastase-induced or calcium chloride-induced AAA models (reviewed in [8]). However, those models produce moderate aortic dilatation in mice and do not induce aortic wall rupture. Finally, while leukocyte infiltration, ECM degradation and medial degeneration are observed in almost all the above-mentioned models, ILT is frequently absent. Thus, there is currently no validated AAA model in mice that reproduces and combines the major features of human AAA: sustained aneurysmal dilatation of the native aorta without false lumen formation, associating ECM degradation, medial degeneration, leukocyte infiltration, ILT formation, and culminating in transmural rupture of the thin aortic wall.

Studies on the mechanisms of aortic aneurysm and dissection have shed light on the importance of TGFβ activity in the maintenance of aortic wall integrity. In mice, genetic disruption of TGFβ signaling in VSMCs early during the disease process promotes the development of aneurysms and dissections in the thoracic aorta [15,16]. Furthermore, blockade of TGFβ activity aggravates ECM degradation, medial degeneration, leukocyte infiltration, and increases the susceptibility to both thoracic and abdominal aortic dissection in mice infused with AngII [17,18]. Finally, promotion of TGFβ activity limits the development and expansion of experimental AAAs [19]. Based on these observations, we hypothesized that TGFβ may be the critical factor that maintains aortic wall integrity in mouse models of 'non-dissecting' AAA (e.g., elastase-induced abdominal aortic injury), and that blockade of TGFβ activity in those settings would aggravate aneurysmal aortic dilatation, induce ILT formation, and promote aortic rupture, thereby reproducing the major features of complicated human AAA.

Materials and Methods

Materials and Methods are available in the online-only Data Supplement.

Results

Inhibition of TGFβ activity induces abdominal aortic rupture after elastase injury

We combined topical application of elastase on the abdominal aorta [20-22] with systemic blockade of TGFβ activity using a neutralizing mouse monoclonal anti-TGFβ [17,18]. As already described [20-22], peri-aortic elastase significantly increased aortic diameter (compared to inactive elastase) as assessed by serial in vivo ultrasound imaging **(Figure 1A** and **1B),** and direct caliper measurement of the external diameter of the aorta at the time of sacrifice **(Figure 1C)**. Interestingly, while aortic dilatation did not progress after day 7 in the group receiving active elastase only **(Figure 1B)**, concomitant inhibition of TGFβ activity dramatically reduced Smad2/3 phosphorylation (**Online-only Data Supplement Figure I**), steadily enhanced aortic enlargement at the site of elastase application throughout the duration of the experiment **(Figure 1B)**, and eventually led to sudden death due to aortic rupture **(Figure 1D** and **1E**, and see below**)**. Staining of aortic sections with Orcein revealed significantly enhanced elastin degradation in mice co-treated with elastase and anti-TGFβ **(Figure 1F)**. These results were reproduced in hyperlipidemic *Apoe*$^{-/-}$ mice (**Online-only Data Supplement Figure IIA**). Systolic blood pressure was not affected by the interventions, and was similar between all experimental groups **(Online-only Data Supplement Figure IIB).** Our data identify a critical role for TGFβ in preserving aortic wall integrity in response to an AAA-inducing insult. The steady increase of AAA diameter over the course of the experiment and the occurrence of AAA rupture in mice treated with anti-TGFβ antibody strongly suggest impaired resolution of the inflammatory process and altered tissue healing in the absence of TGFβ activity (see below). This is further supported by our finding that TGFβ blockade initiated 14 days after peri-aortic elastase application, a stage of non-progressing or resolving AAA, rapidly induced AAA destabilization, and led to fatal aortic rupture (**Online-only Data Supplement Figure III**).

Synchrotron-based ultra-high resolution imaging reveals features of human AAA

In order to characterize this new mouse model of AAA rupture, we used synchrotron-based, ultra-high resolution ex vivo imaging on tissue samples from mice that had been sacrificed at different time points, and assessed in details aortic diameter, elastin degradation, adventitial thickness, and the occurrence of ILT, medial dissection or rupture (**Figure 2** and **Figure 3**). The medial perimeter was highest for locations at which elastin degradation was most outspoken (**Figure 2A** and **2D**, and **online-only Data Supplement Figure IVA**). Both medial perimeter (**Figures 2A-2C**) and elastin degradation (**Figures 2C-2F**) were already elevated 3 days after elastase application, followed by adventitial thickening (**Figures 2G-2I**) and the occurrence of ILT (**Figures 2J-2L)**. In non-ruptured AAA, elastin degradation did not change after day 3 (**Figures 2D, 2E**), while medial perimeter (**Figures 2A, 2B**), adventitial thickening (**Figure 2G, 2H**), and ILT (**Figures 2J, 2K**) still

increased progressively at later time point**s**. We observed that animals with ruptured AAA had substantially larger medial perimeters (**Figures 2C**), extensive elastin degradation (**Figures 2F**), larger ILT volumes (**Figures 2I**), but only moderate although significant increase in adventitial thickness (**Figures 2L**) compared to animals with intact AAA. Synchrotron-based ultra-high resolution analysis throughout the length of the AAA ruled out the occurrence of medial delamination/dissection and attributed fatal aortic death to complete transmural rupture of the media (**Figure 3A**). ILT presence was found both in the main aorta and the side branches (**Figure 3A** and **online-only Data Supplement Figure IVB, IVC**) and was confirmed on aortic sections **(Figure 3B)**. ILT stained positive for platelets (anti-CD41), leukocytes (Hoechst) and fibrin/fibrinogen as shown by confocal microscopy **(Figure 3C)**. Platelets were also found in the aortic wall, in between the medial and adventitial layers, probably due to hemorrhage (**Figure 3D**).

Aortic tissue remodeling in the elastase/anti-TGFβ model

By microscopy on sections from day 14, we confirmed that the combination of elastase and anti-TGFβ significantly enhanced the accumulation of blood/iron in the aortic wall **(Figure 4A)**, and induced profound aortic wall remodeling with SMC loss in the media (**Figure 4B**), adventitial neovascularization (**Figure 4B**), increased accumulation of apoptotic cells (**Figure 4C**), as well as increased MMP activity (**Figure 4D**) and reduced collagen content (**Figure 4E**), as compared to the elastase only group. Proliferation as assessed by Ki67 staining was detected in both immune and stromal cells of vessels subjected to elastase application, but was not different between elastase and elastase + anti-TGFβ groups (**online-only Data Supplement Figure V**).

Inhibition of TGFβ activity increases immune cell accumulation in the aorta after elastase injury

Inflammation is another feature of AAA remodeling and rupture in humans [5]. Using fluorescent microscopy and flow cytometry analysis, we characterized the inflammatory infiltrate present in aortic samples at day 14. TGFβ inhibition after peri-aortic elastase application dramatically increased the accumulation of T cells, macrophages and neutrophils, as compared to aortic samples treated with elastase only **(Figure 5)**. Flow cytometry analysis suggested that macrophages were mostly derived from monocytes, given their high expression of Ly6B (**Figure 5D**), and that the T cell population was composed of both $CD4^+$ and $CD8^+$ cells with an activated phenotype ($CD69^+$) **(Figure 5D)**. We also noticed that, as described in human AAA, the ILT of mice treated with elastase + anti-TGFβ was rich in neutrophils **(Figure 5C)**.

TGFβ blockade limits the accumulation of pro-fibrotic segregated atypical monocytes

Akira and colleagues recently identified a segregated-nucleus-containing atypical monocyte (SatM) subset derived from a committed progenitor downstream of $Ly6B/C^-Fc\varepsilon RI^+$ granulocyte/macrophage progenitors. SatM are $CEACAM1^+MSR1^+Ly6B/C^-F4/80^-MAC1^+$ monocytes that differentiate under the control of C/EBPβ, home to injured tissues during the healing phase and play a crucial role in tissue fibrosis [23]. SatM do not produce TGFβ; however, C/EBPβ deficiency, which eliminates SatM, is associated with substantial

reduction of TGFβ production [23]. Therefore, we tested the impact of TGFβ blockade on the accumulation of SatM after elastase injury. Interesting, we found a substantial reduction of SatM in the bone marrow, blood and aortic wall of mice treated with neutralizing anti-TGFβ antibody and peri-aortic elastase, compared with peri-aortic elastase only (**online-only Data Supplement Figure VI**). Our results support an important role for TGFβ in SatM homeostasis, with potentially important consequences on the healing response.

Monocytes/macrophages are necessary for the induction of AAA rupture after elastase and anti-TGFβ treatment

Given the imbalance between inflammatory monocytes and SatM in mice treated with anti-TGFβ, we hypothesized that monocyte/macrophage depletion using clodronate liposomes would limit disease severity and reduce the occurrence of aortic rupture. Treatment with clodronate liposomes effectively depleted systemic monocytes **(Figure 6A**) and aortic macrophages **(Figure 6B**) in comparison with PBS-loaded liposomes. Monocyte/macrophage depletion did not abrogate aneurysm development (**Figure 6C**) but led to a marked reduction of AAA severity **(Figure 6C)**, and completely protected against AAA rupture (**Figure 6D**). This was associated with a significant reduction of elastin degradation (**Figure 6E**), and increased collagen content (**Figure 6F**).

Role of IL-1β in the initiation versus progression of AAA

To gain more insight into the inflammatory response, we analyzed mRNA expression of cytokines (by Q-PCR) in the aortic tissue and found that both pro-inflammatory (TNF, IL-6, IL-1β, CXCL1) and anti-inflammatory (TGFβ and IL-10) cytokines were induced after elastase injury (**online-only Data Supplement Figure VII**). TNF, IL-1β and CXCL1 reached high levels at D7 but their expression was attenuated at D14. IL6 expression showed a late increase between D7 and D14. IL-10 and TGFβ increased at D7, with variable expression of IL-10 at D14. TGFβ blockade on top of elastase application led to sustained elevations and higher levels of IL-1β, CXCL1 and IL-6 at D14 after aortic injury, but did not alter TNF and IL-10 expression. We also detected a slightly higher aortic TGFβ expression in the elastase + anti-TGFβ at D14, compared with the elastase only group.

The kinetics of IL-1β expression in the aortic wall suggested a differential effect in the initiation versus progression of AAA. In order to directly assess the implication of IL-1β in aortic dilatation and rupture, we compared IL-1β KO and WT mice. We confirmed the absence of IL-1β in the plasma of IL-1β KO mice and found that CXCL1 and IL-10 were also significantly reduced, suggesting a role for IL-1β in the production of these cytokines (**online-only Data Supplement Figure VIIIA**). At day 5 after injury, IL-1β KO mice showed a reduction of circulating neutrophils (**online-only Data Supplement Figure VIIIB**), in accordance with the reduction of plasma CXCL1 levels. As compared to WT mice, IL-1β KO mice showed a marked protection against aortic dilatation (**Figure 7A**), and were totally protected against AAA rupture induced by elastase and anti-TGFβ treatment (**Figure 7B**). Moreover, the injury induced by elastase and TGFβ blockade was dramatically reduced in IL-1β KO mice **(online-only Data Supplement Figure VIIIC-VIIIF)**. To

address the role of IL-1β in the progression and complications of established AAA, we used a mouse monoclonal anti-mouse IL-1β antibody. The antibody significantly blocked the induction of CXCL1 by vascular SMCs in response to recombinant IL-1β in vitro (**online-only Data Supplement Figure IXA**), and significantly reduced plasma levels of CXCL1 and IL-6 in vivo while impairing IL-1β clearance (**online-only Data Supplement Figure IXB**). Importantly, however, neutralization of IL-1β with this monoclonal anti-IL-1β antibody starting at D7 after elastase + anti-TGFβ, did not the limit the progression of established AAA toward fatal rupture (**Figure 7C**). Taken together, our data indicate that IL-1β is important for the initiation of AAA but is dispensable for the progression and/or complications of established AAA.

Discussion

Major features of human AAA include ECM degradation, medial SMC loss and degeneration, infiltration and activation of immune cells, ILT formation, progressive aortic dilatation in the absence of medial dissection, and finally aortic wall rupture. It is noteworthy that despite the variety of experimental models of AAA, none has been reported to combine the major features of human AAA. Most models either induce early medial dissection, not transmural aortic wall rupture, or lead to self-contained aortic dilatation. Furthermore, most models do not induce ILT formation. A rare occurrence of aortic rupture has been reported in elastase-induced AAA in rats, not mice, but those rare ruptures occur very early after elastase application and are due to an overactive exogenous elastase rather than a progressive aneurysmal aortic disease that culminates in aortic wall rupture. Recently, Lu et al. reported the development of a chronic model of AAA in mice after a combination of peri-aortic elastase application and continuous oral administration of the lysyl oxidase inhibitor BAPN [22]. AAA development in that model was associated with thrombus formation and spontaneous rupture. Despite those interesting human-like aneurysm features, the authors provided no evidence for the absence of medial dissection, and there was no evidence that the few late ruptures had arisen from the aortic wall itself; in fact some deaths were attributed to rupture or dissection of small arteries [22]. Moreover, BAPN is known to induce medial dissections, not transmural ruptures, which lead to intramural, not intraluminal, hemorrhage and thrombus formation [11-13].

In contrast to previous models, the AAA model we describe here in detail associates all the major features of human AAA and is potentially of great interest to our understanding of the pathophysiology of AAA development, progression and complications.

It is remarkable to observe that the transition from a model inducing a self-contained aortic dilatation to a human-like model of sustained aneurysmal growth culminating in rupture is due to the blockade of a single cytokine, TGFβ. This supports a critical role of TGFβ signaling in the maintenance of aortic wall integrity and the protection against AAA progression and complications. Mutations in the TGFβ signaling pathway are responsible for severe forms of thoracic aortic aneurysms and dissections in humans [24], and some studies reported associations between single-nucleotide polymorphisms in the TGFβ signaling components and AAA [25]. Moreover, human AAA biopsies frequently show loss of one copy of TGFβ receptor type 2 exon 8 in association with a substantial reduction of gene expression, suggesting an acquired impairment in the TGFβ pathway and local down-regulation of TGFβ signaling [26]. The major sources of TGFβ during AAA development remain to be identified. Immune cells, VSMCs, (myo)fibroblasts, and platelets may all contribute to TGFβ production.

How does TGFβ activity control AAA dilatation and propensity to rupture? TGFβ is well known to control major biological processes involved in AAA, including ECM remodeling, VSMC survival and proliferation, as well as the activation of the immuno-inflammatory response [25]. We show here that at least some of the protective effect occurs through the control of the innate immune response, and more particularly the balance between inflammatory monocytes/macrophages and pro-fibrotic SatM. The specific role of the latter monocyte subset will require further investigation. Moreover, other innate

immune cells like neutrophils, or adaptive immune cells like T cells, may cooperate with monocytes/macrophages, and probably contribute to the process. Note that our study does not exclude a role for TGFβ activity in vascular cells and (myo)fibroblasts. However, deletion of TGFβ receptor signaling in VSMC did not lead to aggravation of AAA after elastase application in mice [27]. The latter result is surprising given the major role of VSMC-restricted TGFβ signaling in the protection against thoracic aortic aneurysms [15,16,28].

Our study identifies IL-1β as an important cytokine involved in the prevention of AAA development, which is an agreement with previous studies performed in less severe models of the disease [29]. Surprisingly, however, IL-1β blockade did not affect the progression of established AAA toward rupture, suggesting a limited role (if any) of IL-1β in advanced stages of the disease. The role of IL-1 pathway in human AAA is not well understood. Genetic upregulation of IL-1 receptor antagonist in humans is associated with increased, not reduced, susceptibility to AAA [30]. Moreover, a recent placebo-controlled randomized trial failed to show any benefit of Canakinumab (a neutralizing monoclonal anti-IL-1β antibody) on AAA progression in patients with 'small' AAAs (between 40 and 50 mm) [31]. The trial included a limited number of patients in each group (31 Canakinumab and 33 placebo), and only 2/3 of patients completed the 12 months treatment period. These unexpected human data are in disagreement with previous mouse data that suggested a detrimental role for IL-1 signaling in the progression of AAA, using the elastase model [29]. However, they appear to be in agreement with our findings of a limited role of IL-1β in established AAA, using the present elastase + anti-TGFβ model, further highlighting the clinical translational relevance of this new mouse model.

Another important point to consider is the chronicity and sustainability of AAA development and growth over time. Most available experimental models of 'non-dissecting' AAA induce a development of AAA over 7 days and are rapidly self-contained with no or very little AAA progression thereafter; in fact, they tend to heal with time in the absence of sustained injury. The elastase + BAPN model described recently allows the development of a chronic aortic aneurysm and is worth of further consideration [22]. However, there is no solid evidence yet that it is not driven by early medial dissection or that sudden death is due to true aortic wall rupture. In this context, our identification of TGFβ as a critical mediator of AAA healing is likely to open new avenues for the development of chronic models of non-dissecting AAA characterized by an impaired healing process and sustained growth, until aortic rupture. Our current elastase/anti-TGFβ model produces a human-like AAA and a high percentage of AAA rupture within 14 days. We believe that this model can be adapted to produce a non-resolving inflammation that will sustain AAA growth over a longer period, for example through controlled blockade of TGFβ over time (varying the frequency and dose of anti-TGFβ), better mimicking the progression of human AAA. It is expected that in such a chronic 'smoldering' model, the pathogenic mechanisms of AAA growth may differ from our current understanding of disease pathogenesis.

Finally, the new model described here may be useful to address the role of specific features of AAA, e.g. ILT formation, in AAA progression and susceptibility to rupture. Moreover, it will be interesting to examine if blockade

of TGFβ activity may be useful in promoting features of human-like AAA in other experimental models, like the CaCl2 model.

In conclusion, we have shown that current experimental mouse models of AAA can be improved to better reproduce major features of human AAA, and may be harnessed to predict response to therapy in the human disease setting. We expect that optimized models will provide a better understanding of the pathophysiology of AAA, and will be useful to identify and test new and relevant therapeutic targets.

Acknowledgements
We gratefully acknowledge the assistance of the Department of Clinical Biochemistry, University of Cambridge for the analysis of serum biochemical parameters, and the Department of Medicine Phenotyping hub, University of Cambridge for assistance with flow cytometry. We thank Dr. Yoichiro Iwakura (Center for Experimental Medicine, Institute of Medical Science, University of Tokyo, Tokyo, Japan) for providing the IL-1β deficient mice.

Sources of Funding
This work was supported by the British Heart Foundation, and the European Research Council (to Z.M.).

Disclosures
None.

References

1. Jacomelli J, Summers L, Stevenson A, Lees T, Earnshaw JJ. Impact of the first 5 years of a national abdominal aortic aneurysm screening programme. Br J Surg 2016;103:1125-1131.
2. Moll FL, Powell JT, Fraedrich G, Verzini F, Haulon S, Waltham M, van Herwaarden JA, Holt PJ, van Keulen JW, Rantner B, Schlosser FJ, Setacci F, Ricco JB, European Society for Vascular S. Management of abdominal aortic aneurysms clinical practice guidelines of the European society for vascular surgery. Eur J Vasc Endovasc Surg 2011;41 Suppl 1:S1-S58.
3. Brady AR, Thompson SG, Fowkes FG, Greenhalgh RM, Powell JT, Participants UKSAT. Abdominal aortic aneurysm expansion: risk factors and time intervals for surveillance. Circulation 2004;110:16-21.
4. Patel R, Sweeting MJ, Powell JT, Greenhalgh RM, investigators Et. Endovascular versus open repair of abdominal aortic aneurysm in 15-years' follow-up of the UK endovascular aneurysm repair trial 1 (EVAR trial 1): a randomised controlled trial. Lancet 2016;388:2366-2374.
5. Nordon IM, Hinchliffe RJ, Loftus IM, Thompson MM. Pathophysiology and epidemiology of abdominal aortic aneurysms. Nat Rev Cardiol 2011;8:92-102.
6. Nienaber CA, Clough RE. Management of acute aortic dissection. Lancet 2015;385:800-811.
7. Sakalihasan N, Limet R, Defawe OD. Abdominal aortic aneurysm. Lancet 2005;365:1577-1589.
8. Senemaud J, Caligiuri G, Etienne H, Delbosc S, Michel JB, Coscas R. Translational Relevance and Recent Advances of Animal Models of Abdominal Aortic Aneurysm. Arterioscler Thromb Vasc Biol 2017;37:401-410.
9. Daugherty A, Manning MW, Cassis LA. Angiotensin II promotes atherosclerotic lesions and aneurysms in apolipoprotein E-deficient mice. J Clin Invest 2000;105:1605-1612.
10. Trachet B, Fraga-Silva RA, Piersigilli A, Tedgui A, Sordet-Dessimoz J, Astolfo A, Van der Donckt C, Modregger P, Stampanoni MF, Segers P, Stergiopulos N. Dissecting abdominal aortic aneurysm in Ang II-infused mice: suprarenal branch ruptures and apparent luminal dilatation. Cardiovasc Res 2015;105:213-222.
11. Kurihara T, Shimizu-Hirota R, Shimoda M, Adachi T, Shimizu H, Weiss SJ, Itoh H, Hori S, Aikawa N, Okada Y. Neutrophil-derived matrix metalloproteinase 9 triggers acute aortic dissection. Circulation 2012;126:3070-3080.
12. Jia LX, Zhang WM, Zhang HJ, Li TT, Wang YL, Qin YW, Gu H, Du J. Mechanical stretch-induced endoplasmic reticulum stress, apoptosis and inflammation contribute to thoracic aortic aneurysm and dissection. J Pathol 2015;236:373-383.
13. Ren W, Liu Y, Wang X, Jia L, Piao C, Lan F, Du J. beta-Aminopropionitrile monofumarate induces thoracic aortic dissection in C57BL/6 mice. Sci Rep 2016;6:28149.
14. Liu S, Xie Z, Daugherty A, Cassis LA, Pearson KJ, Gong MC, Guo Z. Mineralocorticoid receptor agonists induce mouse aortic aneurysm formation and rupture in the presence of high salt. Arterioscler Thromb Vasc Biol 2013;33:1568-1579.

15. Li W, Li Q, Jiao Y, Qin L, Ali R, Zhou J, Ferruzzi J, Kim RW, Geirsson A, Dietz HC, Offermanns S, Humphrey JD, Tellides G. Tgfbr2 disruption in postnatal smooth muscle impairs aortic wall homeostasis. J Clin Invest 2014;124:755-767.
16. Hu JH, Wei H, Jaffe M, Airhart N, Du L, Angelov SN, Yan J, Allen JK, Kang I, Wight TN, Fox K, Smith A, Enstrom R, Dichek DA. Postnatal deletion of the type II transforming growth factor-beta receptor in smooth muscle cells causes severe aortopathy in mice. Arterioscler Thromb Vasc Biol 2015;35:2647-2656.
17. Wang Y, Ait-Oufella H, Herbin O, Bonnin P, Ramkhelawon B, Taleb S, Huang J, Offenstadt G, Combadiere C, Renia L, Johnson JL, Tharaux PL, Tedgui A, Mallat Z. TGF-beta activity protects against inflammatory aortic aneurysm progression and complications in angiotensin II-infused mice. J Clin Invest 2010;120:422-432.
18. Chen X, Rateri DL, Howatt DA, Balakrishnan A, Moorleghen JJ, Cassis LA, Daugherty A. TGF-beta neutralization enhances AngII-induced aortic rupture and aneurysm in both thoracic and abdominal regions. PLoS One 2016;11:e0153811.
19. Dai J, Losy F, Guinault AM, Pages C, Anegon I, Desgranges P, Becquemin JP, Allaire E. Overexpression of transforming growth factor-beta1 stabilizes already-formed aortic aneurysms: a first approach to induction of functional healing by endovascular gene therapy. Circulation 2005;112:1008-1015.
20. Bhamidipati CM, Mehta GS, Lu G, Moehle CW, Barbery C, DiMusto PD, Laser A, Kron IL, Upchurch GR, Jr., Ailawadi G. Development of a novel murine model of aortic aneurysms using peri-adventitial elastase. Surgery 2012;152:238-246.
21. Busch A, Holm A, Wagner N, Ergun S, Rosenfeld M, Otto C, Baur J, Kellersmann R, Lorenz U. Extra- and intraluminal elastase induce morphologically distinct abdominal aortic aneurysms in mice and thus represent specific subtypes of human disease. J Vasc Res 2016;53:49-57.
22. Lu G, Su G, Davis JP, Schaheen B, Downs E, Roy RJ, Ailawadi G, Upchurch GR, Jr. A novel chronic advanced stage abdominal aortic aneurysm murine model. J Vasc Surg 2017;10.1016/j.jvs.2016.07.105.
23. Satoh T, Nakagawa K, Sugihara F, Kuwahara R, Ashihara M, Yamane F, Minowa Y, Fukushima K, Ebina I, Yoshioka Y, Kumanogoh A, Akira S. Identification of an atypical monocyte and committed progenitor involved in fibrosis. Nature 2017;541:96-101.
24. Gillis E, Van Laer L, Loeys BL. Genetics of thoracic aortic aneurysm: at the crossroad of transforming growth factor-beta signaling and vascular smooth muscle cell contractility. Circ Res 2013;113:327-340.
25. Wang Y, Krishna S, Walker PJ, Norman P, Golledge J. Transforming growth factor-beta and abdominal aortic aneurysms. Cardiovasc Pathol 2013;22:126-132.
26. Biros E, Walker PJ, Nataatmadja M, West M, Golledge J. Downregulation of transforming growth factor, beta receptor 2 and Notch signaling pathway in human abdominal aortic aneurysm. Atherosclerosis 2012;221:383-386.
27. Gao F, Chambon P, Offermanns S, Tellides G, Kong W, Zhang X, Li W. Disruption of TGF-beta signaling in smooth muscle cell prevents elastase-

induced abdominal aortic aneurysm. Biochem Biophys Res Commun 2014;454:137-143.
28. Wei H, Hu JH, Angelov SN, Fox K, Yan J, Enstrom R, Smith A, Dichek DA. Aortopathy in a mouse model of Marfan syndrome is not mediated by altered transforming growth factor beta signaling. J Am Heart Assoc 2017;6.
29. Johnston WF, Salmon M, Su G, Lu G, Stone ML, Zhao Y, Owens GK, Upchurch GR, Jr., Ailawadi G. Genetic and pharmacologic disruption of interleukin-1beta signaling inhibits experimental aortic aneurysm formation. Arterioscler Thromb Vasc Biol 2013;33:294-304.
30. Chambers JC, Loh M, Lehne B, et al. Epigenome-wide association of DNA methylation markers in peripheral blood from Indian Asians and Europeans with incident type 2 diabetes: a nested case-control study. Lancet Diabetes Endocrinol 2015;3:526-534.
31. ClinicalTrials.Gov. https://clinicaltrials.gov/ct2/show/NCT02007252?term=ACZ885&rank=5.)

Highlights

- Endogenous TGFβ activity is required for the healing of AAA.
- Systemic blockade of TGFβ in the elastase-AAA model in mice induces a transition from a self-contained aortic dilatation to a model of sustained aneurysmal growth, associated with the formation of an intra-luminal thrombus (ILT), and culminates in fatal transmural aortic wall rupture.
- Early blockade of IL1β limits AAA severity. However, blockade of IL1β after disease initiation has no effect on AAA progression to rupture.
- TGFβ blockade may be harnessed to generate new models of AAA with better relevance to the human disease.

Figure Legends

Figure 1. Blockade of TGFβ activity in mice increases the severity of elastase-induced AAA and induces aortic rupture.
(A) and (B)- Representative ultrasound images at day 14 (D14), and quantification of lumen dilation over time in the 3 groups (n=9/group). Two way ANOVA and Tukey post-hoc analysis. Red stars: ***p<0.001 day 7 or day 14 vs day 0; Black stars: ***p<0.001 Elastase vs Elastase + anti-TGFβ at day 14. (C)- Representative images and quantification of external aortic diameter (mm) by caliper at day 14 (n=9/group; Kruskal-Wallis + uncorrected Dunn's test). *p<0.05 Inactive elastase vs elastase; ***p<0.001 Inactive elastase vs Elastase + anti-TGFβ and Elastase vs Elastase + anti-TGFβ (D)- Survival curve (n=9/group; Log Rank, Mantel-Cox) and representative image of aortic rupture in situ (red arrow shows the hematoma) after necropsy (E). **p<0.01 Elastase vs Elastase + anti-TGFβ (F)- Representative images of Orcein staining and quantification of elastin degradation at day 14 (n=9/group). Kruskal-Wallis + uncorrected Dunn's test, *p<0.05 Inactive elastase vs elastase and Elastase vs Elastase + anti-TGFβ, ***p<0.001 Inactive elastase vs Elastase + anti-TGFβ.

Figure 2. Synchrotron-based analysis of elastase-induced injury in the presence of anti-TGFβ.
Digital analysis of medial aortic perimeter (A-C), elastin degradation (D-F), adventitial thickening (G-I) and intraluminal thrombosis (J-L) after Synchrotron imaging. (A, D, G, J)- Left dotted line represents the location of the left renal artery; right (colored) dotted lines represent the iliac bifurcation. Note that the distance between the left renal artery and the iliac bifurcation increased with the progression of AAA. (C, F, I, L)- No aortic rupture: live mice between D7 and D14 (n=12); Aortic rupture: death occurred between D6 and D14 (n=11). Mann-Whitney test. *p<0.05, ***p<0.001 No aortic rupture vs aortic rupture.

Figure 3. Blockade of TGFβ activity after elastase injury induces elastic degradation, adventitial remodeling, aortic rupture and intraluminal thrombus formation.
(A)- Representative 3D segmentation and raw synchrotron pictures of a normal aorta (top row), an aneurysmal aorta (middle row) and a ruptured aneurysm (bottom row). Elastic laminae, adventitial remodeling and intraluminal thrombus (ILT) formation are color-coded. (B)- Representative images of ILT analysis in the three groups and quantification of the presence of ILT. Chi2 test, *p<0.05 Elastase vs Elastase + anti-TGFβ. (C)- Characterization of ILT by immunofluorescent staining showing the accumulation of platelets (CD41-green), fibrin/fibrinogen (Red) and cells (Hoechst+) in the lumen side of the aortic wall. (D)- Representative picture showing the accumulation of platelets in the aortic wall and the formation of neovessels (CD31+) on serial sections.

Figure 4. Blockade of TGFβ activity after elastase injury reproduces histological features of human AAA.

Aortic cryosections from mice at day 14 (n=9/group) after surgery were stained for iron accumulation (A, Perl's staining), the presence of SMC to assess neovascularization and medial SMCs (αSMA staining, B), apoptosis (TUNEL staining, C), gelatinase activity (DG-gelatin, D) and collagen (Sirius red staining, E). Each staining was quantified in the 3 groups of mice (n=9/group). Kruskal-Wallis + uncorrected Dunn's test.
In A, ***p<0.001 Inactive elastase vs Elastase + anti-TGFβ, **p<0.01 Elastase vs Elastase + anti-TGFβ. In B, ***p<0.001 Inactive elastase vs Elastase + anti-TGFβ, *p<0.05 Elastase vs Elastase + anti-TGFβ and Inactive elastase vs Elastase. In C, ***p<0.001 Inactive elastase vs Elastase + anti-TGFβ, **p<0.01 Elastase vs Elastase + anti-TGFβ. In D, *p<0.05 Inactive elastase vs Elastase + anti-TGFβ. In E, *p<0.05 Elastase vs Elastase + anti-TGFβ.

Figure 5. Blockade of TGFβ activity sustains elastase-induced inflammation in the aorta.
Aortic cryosections from mice at day 14 (n=9/group) after surgery were stained for T cells (A), macrophages (B) and neutrophils (C). (A-C)- Quantifications are shown at day 14 (n=9/group). Kruskal-Wallis + uncorrected Dunn's test. In C, the dotted line circles the intraluminal thrombus. (D, E)- Flow analysis of aortic $CD45^+$ cells at day 14 (n=4/group). Representative flow chart showing neutrophils, macrophages and T cell analysis in the aorta of mice treated with elastase or elastase + anti-TGFβ (D), and distribution of immune cells in the aorta of each group (E).
In A, ***p<0.001 Inactive elastase vs Elastase + anti-TGFβ, *p<0.05 Elastase vs Elastase + anti-TGFβ. In B ***p<0.001 Inactive elastase vs Elastase + anti-TGFβ, *p<0.05 Elastase vs Elastase + anti-TGFβ and Inactive elastase vs Elastase. In C, ***p<0.001 Inactive elastase vs Elastase + anti-TGFβ, **p<0.01 Elastase vs Elastase + anti-TGFβ.

Figure 6. Depletion of monocytes/macropahges using clodronate liposomes in mice treated with elastase + anti-TGFβ prevents aortic rupture.
(A)- Representative flow data of macrophages in the spleen 5 days after liposome injection (n=5/group). (B)- Representative immunofluorescent staining of macrophages in the aorta on day 14 after surgery (n=7-9/group). (C)- Representative macroscopic picture and quantification of aortic perimeter of aorta at day 14 after surgery (n=7-9/group). Mann-Whitney test. *p<0.05 Liposome-PBS vs Liposome-clodronate. (D)- Survival curves of mice injected with liposomes (n=7-9 mice/group). Log Rank, Mantel-Cox test. **p<0.01 Liposome-PBS vs Liposome-clodronate. (E, F)- Analysis of elastin and collagen degradation using Orcein staining (E) and Sirius Red (F), respectively. Mann-Whitney test (n=7-9 mice/group). In E and F, *p<0.05 Liposome-PBS vs Liposome-clodronate.

Figure 7. Blocking IL-1β does not prevent aortic rupture of established AAA.
(A)- Representative macroscopic picture and quantification of aortic perimeter of aorta at day 14 after surgery (n=10-12/group). Mann-Whitney test. (B)-

Survival curves of mice (n=10-12/group). Log Rank, Mantel-Cox test. (C)- WT mice were injected (or not) on day 7 with a neutralizing mouse anti-mouse IL-1β antibody Injections were repeated on days 9 and 11. Survival curves of mice (n=12/group). Log Rank, Mantel-Cox test. In A and B, ***p<0.001 WT vs IL-1β KO.

Figures

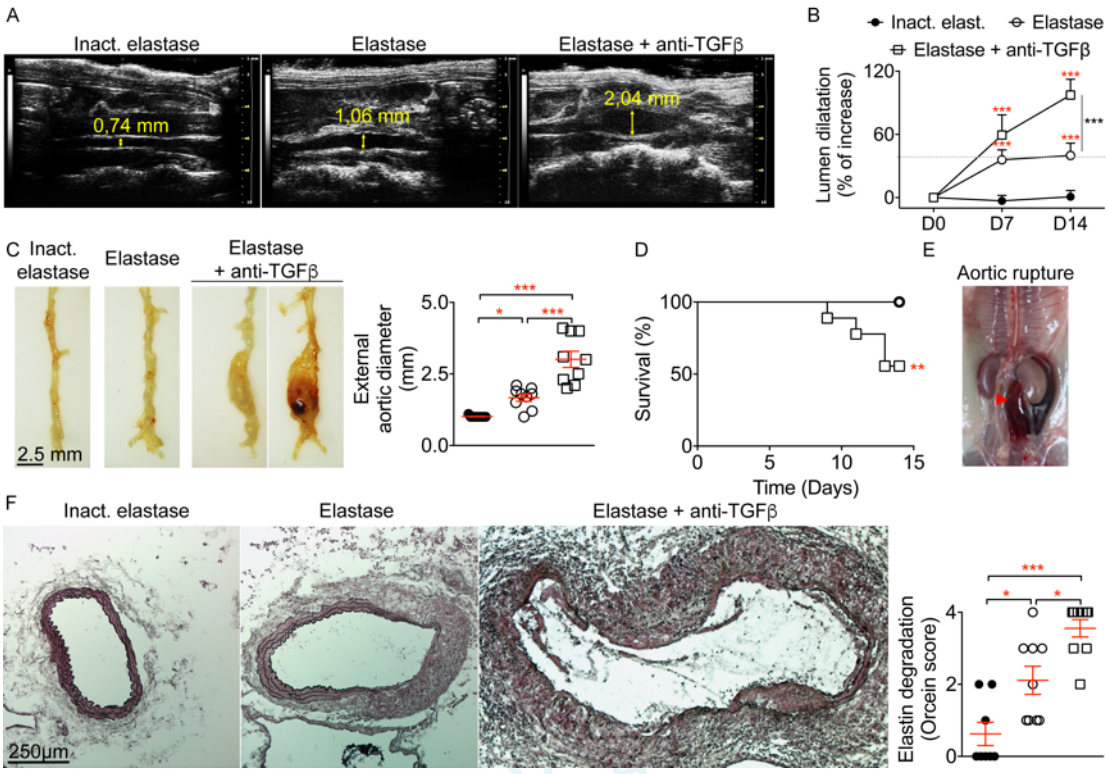

Figure 1

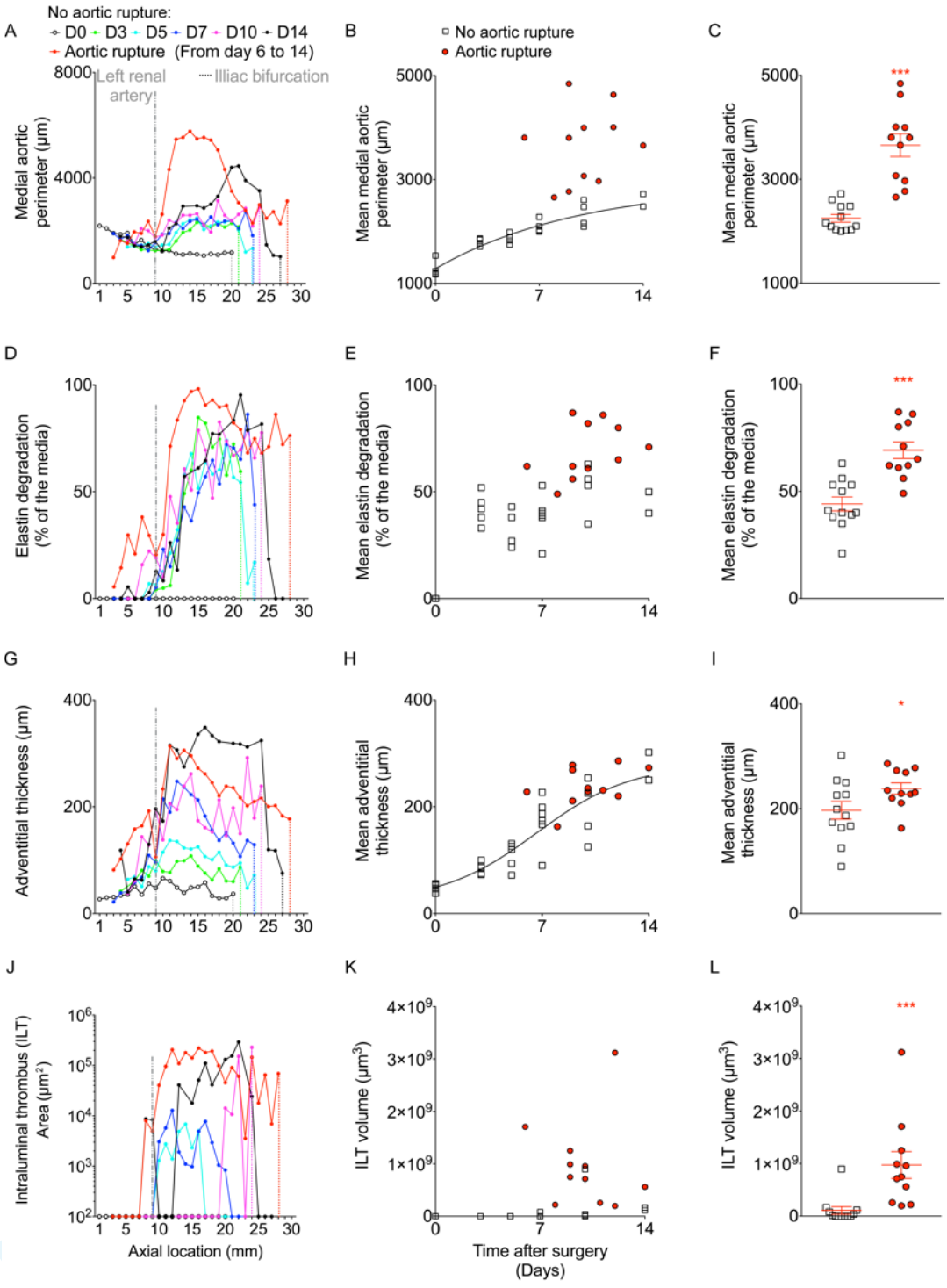
A
No aortic rupture:
D0 D3 D5 D7 D10 D14
Aortic rupture (From day 6 to 14)
Left renal artery
Illiac bifurcation
Medial aortic perimeter (µm)
B
No aortic rupture
Aortic rupture
Mean medial aortic perimeter (µm)
C
***
Mean medial aortic perimeter (µm)
D
Elastin degradation (% of the media)
E
Mean elastin degradation (% of the media)
F
***
Mean elastin degradation (% of the media)
G
Adventitial thickness (µm)
H
Mean adventitial thickness (µm)
I
*
Mean adventitial thickness (µm)
J
Intraluminal thrombus (ILT) Area (µm²)
Axial location (mm)
K
ILT volume (µm³)
Time after surgery (Days)
L
***
ILT volume (µm³)

Figure 2

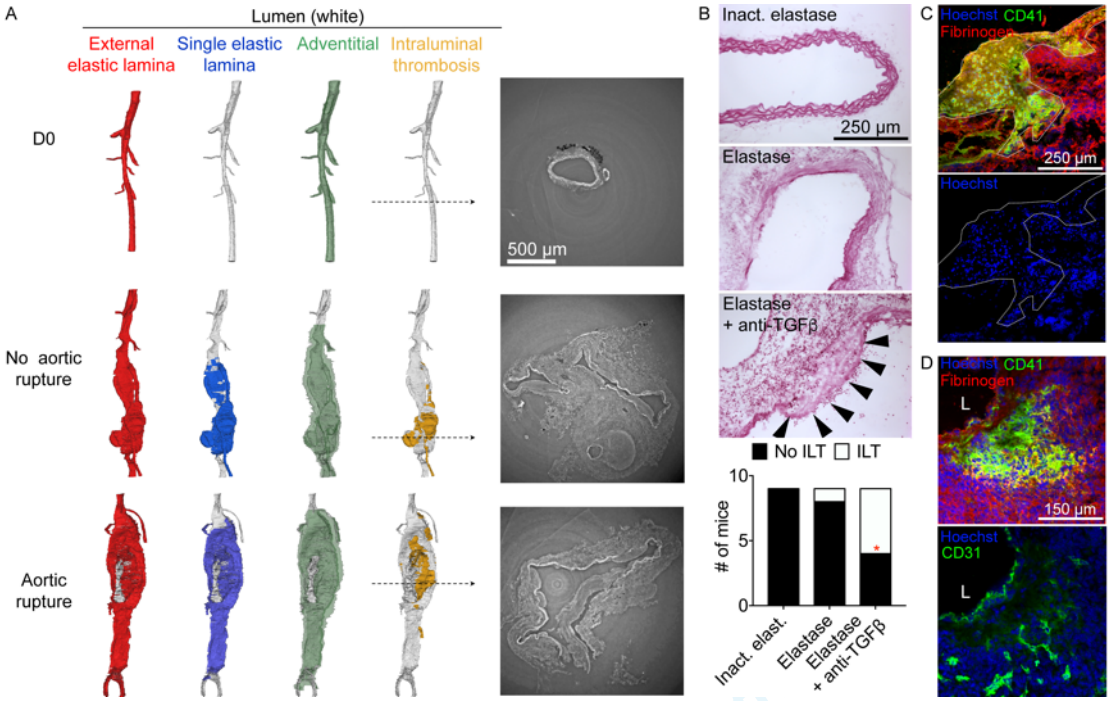

Figure 3

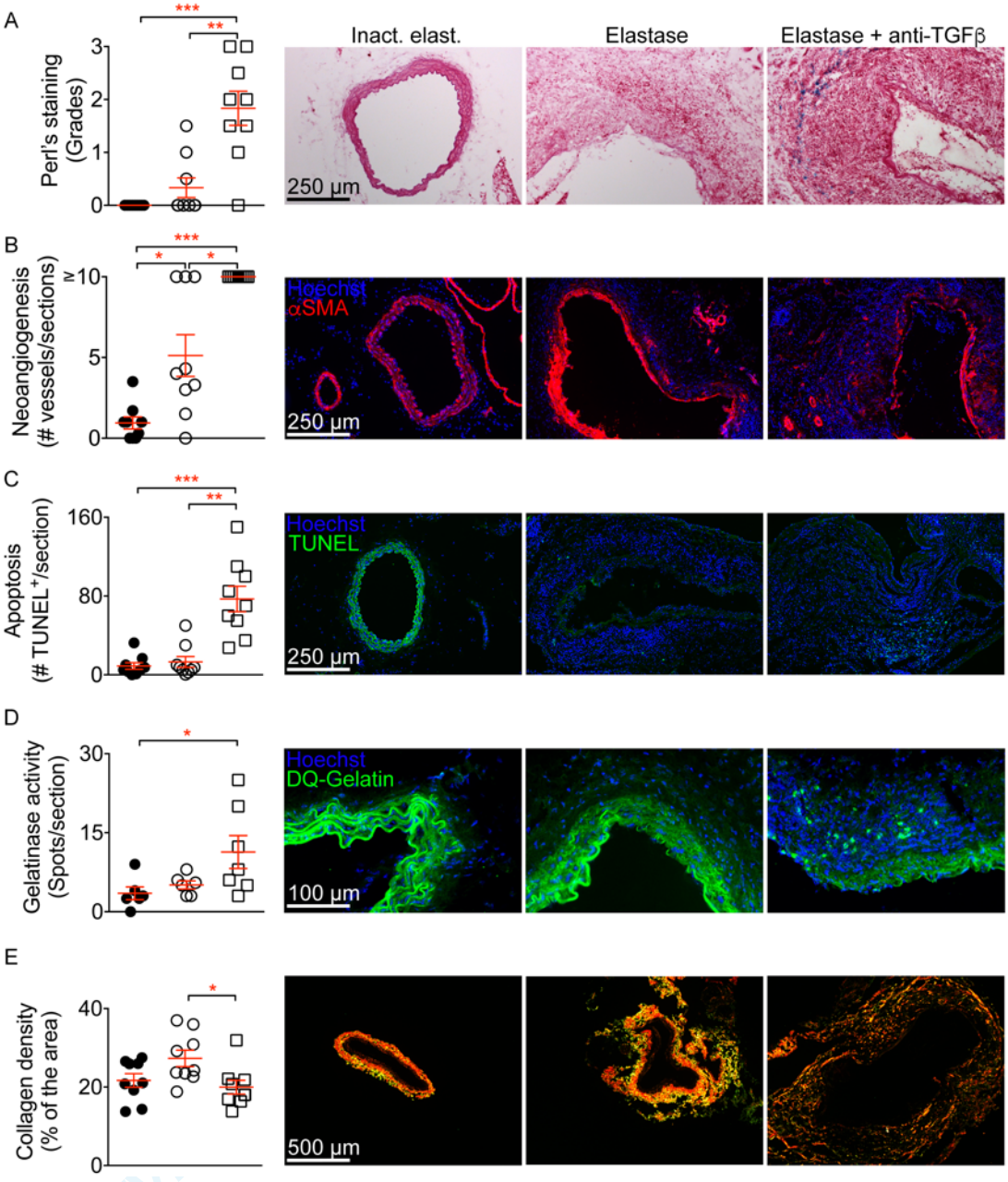

Figure 4

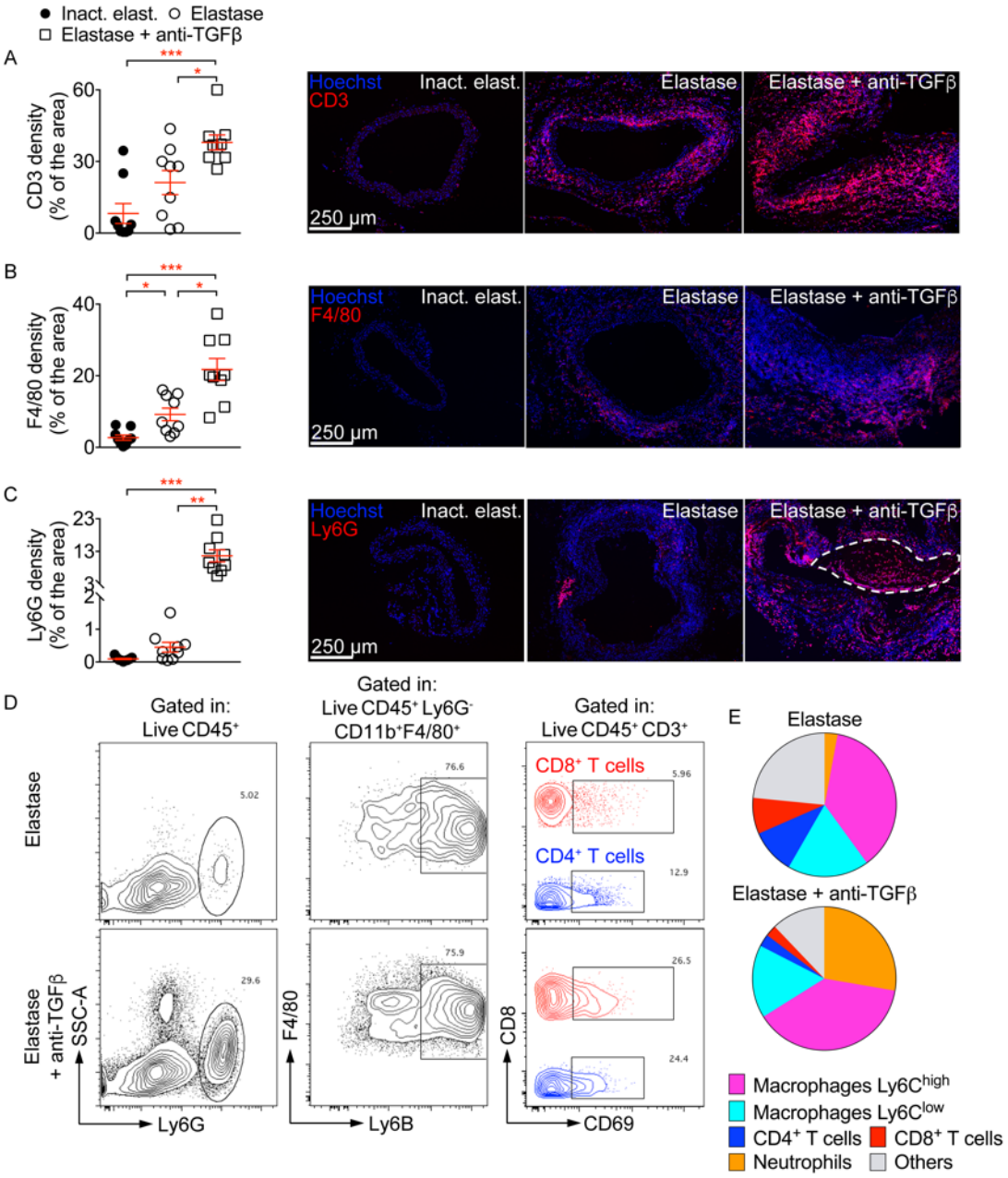

Figure 5

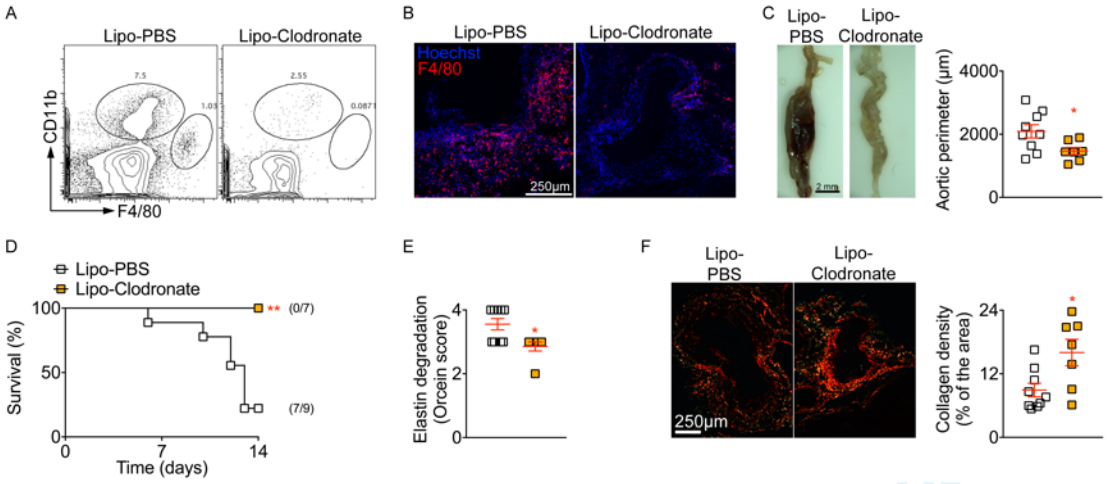

Figure 6

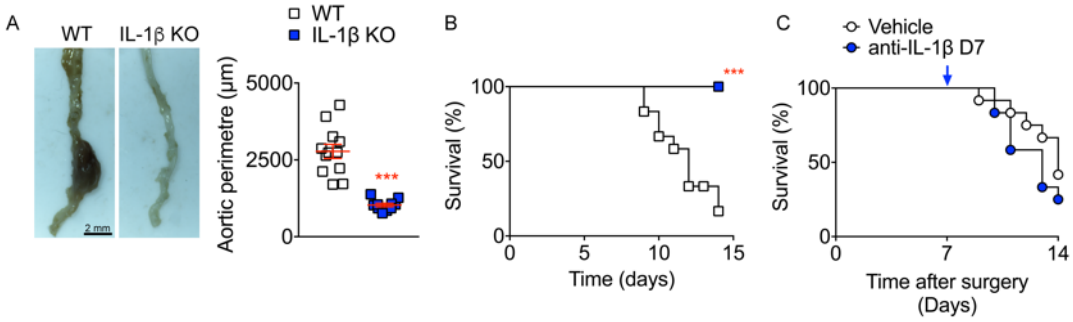

Figure 7